Two-Dimensional Numerical Simulation of Flame Acceleration and Deflagration-to-Detonation Transition in Channels with Obstacles: Effects of Blockage Ratio and Chanel Size

Kanta Iwasaki[1], Ayu Ago[1], Nobuyuki Tsuboi[1], Kohei Ozawa[1], A. Koichi Hayashi[2]

[1]Department of Mechanical and Control Engineering, Kyushu Institute of Technology, Kitakyushu, Fukuoka, Japan
[2]Department of Mechanical Engineering, Aoyama Gakuin University, Sagamihara, Kanagawa, Japan

1 Introduction

DDT (Deflagration to Detonation Transition) is one of the methods to initiate detonation by small energy. It is known in early researches [1-2] that DDT in a channel is promoted by installing obstacles. Dorofeev et al. [3] performed excellent experiment on DDT with obstacles. They introduced the characteristic size L and showed that detonation occurred when the value obtained by dividing L by the detonation cell size λ was larger than 7. Goodwin et al. [4] investigated the effects of blockage ratio on DDT in channels have convex obstacles by the two-dimensional numerical analysis using a one-step reaction model. In the report, they explained the differences in the mechanism of detonation occurrence by dividing blockage ratio (BR) into three types (BR = 0.8, BR = 0.3-0.5, BR = 0.05-0.2). Their simulation indicated that too high blockage ratios (e.g, BR = 0.8) did not reduce detonation transition distance because high obstacles prevent flame from proceeding. They also performed the three-dimensional simulation and obtained the same mechanism of detonation as the two-dimensional simulation. However, the time and position of DDT occurred were different. In the three-dimensional simulation, flame accelerated greatly and resulted in early detonation transition than in the two-dimensional simulation. Maeda et al. [5] made experiments to visualize DDT in a channel with obstacles and photographed the phenomena at the side views and the bottom views of the channel. The experiments showed that the DDT distances were the same whether there are obstacles in the downstream or not. Moreover, when the flame propagating in the depth direction reached the side wall, a local explosion occurred at an unreacted gas pocket and transited to detonation.

Though there is a lot of research about DDT, the mechanisms and prediction of detonation transition distance are not fully understood. Regarding numerical analysis, many researchers use simplified one-step reaction model rather than detailed reaction model. However, there is a report [6] saying that the simulation by one-step reaction model may make incorrect conclusions quantitatively because turbulence in chemically reactive flows is affected by the reactions. Ago et al. [7] performed the two-dimensional simulation on DDT in channels with obstacles for BR = 0.3 and 0.45 using a detailed reaction model. The detonation transition

Correspondence to: iwankov103@gmail.com

for BR = 0.45 was delayed than for BR = 0.3. They obtained results that agree well with the mechanism of local detonation in the experiment of DDT. Although there are many studies the mechanism of detonation transition by numerical simulations, there are few studies that whether flame propagation by numerical analysis reproduces experimental flame propagation. This research investigates flame propagation and local explosions in a channel filled with hydrogen/oxygen stoichiometric mixture and installed square obstacles by using the two-dimensional simulation using a detailed reaction model. Furthermore, we estimate differences between the three-dimensional experiments performed by Maeda et al. [5] and the present two-dimensional simulations.

2 Numerical Methods and Simulation Conditions

The governing equations are the two-dimensional compressible Navier-Stokes equations including mass conservation of nine chemical species. AUSMDV (Advection Upstream Splitting Method flux Difference and flux Vector scheme) [8] with the second-order MUSCL (Monotonic Upstream-Centered Scheme for Conservation Laws) [9] and minmod-limiter are applied for the convection terms. The time integration method uses the third-order TVD Runge-Kutta (Total Variation Diminishing Runge-Kutta) method. [10] The source term is integrated by the point implicit method. The detailed reaction model UT-JAXA [11] is adopted with nine species (H_2, O_2, N_2, O, H, OH, HO_2, H_2O_2, and H_2O) and twenty-one elementary reactions.

Figure 1 shows one of the frames of calculation grids used in the present simulation. The calculation area is divided into twenty-one zones and these zones are reproduced as a channel with ten obstacles equally spaced. This is because this simulation is performed using an in-house code to produce grid system easily. One of the channel sizes has a height of 4.25 mm and the width of 33.5 mm, which are the one-twentieth scale of the experimental equipment used by Maeda et al. [5]. This set of the frames uses 5 μm orthogonal grids. The distance from the left end to the first obstacle is 1.0 mm and the distance between obstacles is 3.0 mm. The width of obstacles is 0.25 mm and the height was set by three patterns: BR (blockage ratio) of 0.06, 0.12 and 0.18. The other size is the one-tenth scale of the experimental one with 10 μm orthogonal grids for BR of 0.18. In Fig. 1, two adjacent zones are arranged so that eleven grid points in the longitudinal direction overlap each other to interpolate physical values calculated in each zone and to calculate twenty-one zones as one area. The total number of grid points is about 5.7 million in any frames. For the right-side downstream boundary, the outflow condition of Gamezo et al. [12] is adopted to avoid the reflection. The other boundary conditions are set as the adiabatic non-slip wall condition. The ambient region is filled with stoichiometric hydrogen/oxygen premixed gas with the pressure of 70 kPa and the temperature of 293 K, respectively. The ignition area is a semicircle with a radius of 0.25 mm on the 1.75 mm from the bottom in the left end of the calculation area. The initial pressure is 3 atm and the temperature is 3000 K in the ignition area.

3 Results and Discussions

3.1 Effects of obstacles height

Figure 2 shows the flame velocities at the position from left-side of channels for various obstacle heights. The channels are the one-twentieth scale of experimental equipment [5]. Since the propagation velocities did not reach the CJ velocity (= 2840 m/s), the deflagration did not transfer to the detonation for any obstacle heights. In Fig. 2, it is found that the amplitude of velocity oscillation and velocity increase is larger when obstacles height increases.

Figure 3 (Left) shows the flame propagation for BR of 0.06 near the fifth obstacle. When the flame front passes over the obstacles, the flame tip diffracted. However, the diffracted flame was small and disappeared without interfering the flame in the main flow since the height of obstacles is low. Therefore, a large increase in heat of combustion or flame acceleration was not observed for this case.

For BR of 0.18, flames were more disturbed by the obstacles than the case for BR of 0.06. Figure 3 (Right) show that flames passed the seventh obstacle and diffract for BR of 0.18. In those cases, multiple vortexes created by the diffracted flame climbed up above the obstacle and pushed the mainstream flame out. Then, the vortices spread out and disappeared. In Fig. 3 (Right) for BR of 0.18, the shock waves (**SW**) was generated upward when the vortices rolled up. The shock waves reflected on the up-side wall of channel (**RS**) and the flame temperature increased. These results indicate that higher obstacles disturbed the flame propagation and induced the shock waves crossing the channel, which lead to the enhancement and acceleration of the combustion reaction. However, in each BR no local strong explosion was observed and the flame did not transit to detonation.

3.2 Effects of channel size

Figure 4 shows the flame velocity from left-side of channel for BR of 0.18. The distance on the horizontal axis in the graph is normalized. In this case, the propagation velocity did not reach the CJ velocity and the DDT process was not observed. The time-averaged acceleration of the flame is approximately the same as that at the one-twentieth scale in Fig. 4. The flame propagates similarly to that shown in Fig. 3 (c). However, a small local explosion was observed near the 7th obstacles at one-tenth the size. In Figure 5, the case when a local explosion occurred is arranged in chronological order. The flame is diffracted and disturbed at seventh obstacle proceeded in the upstream direction. The flame 1 (**F1**) flows into the unburned area in front of seventh obstacle which is pushed by the reflected shock wave (**RS**). The flame 2 (**F2**) on the bottom of the channel also flows into that area. As a result, the unburned area is compressed and a local explosion occurs. However, the explosion is small so that a detonation wave (**DW**) becomes into shock wave (**SW**) instantly since it is surrounded by the burned gas. The flame propagates as a deflagration without transition to detonation.

3.3 Comparison with experiment results

In the experiments by Maeda et al. [5], the local explosions occurred behind the third or fourth obstacle at any cases height, and the flames transfer to detonation. However, the DDT did not occur within the calculation domain in the present two-dimensional numerical analysis using the channels scaled down from the actual experimental setup. Comparing with the propagation velocity of flames in Fig. 5, the experiments have reached speeds of 400 m/s or more between third obstacle and fourth obstacle. However it has not reached 400 m/s in the present numerical simulation. It seems that the large acceleration of flame is related to the early detonation transition. Furthermore, cellular structure due to flame instability was observed in experiment, but the flame surface was smooth in simulations. We need to investigate the effect of flame instability. In the future, it is necessary to verify the flame propagation by the three-dimensional simulations with the experimental size because it is difficult to obtain similar results in two-dimensional simulations like a three-dimensional experiment considering the depth direction.

4 Conclusions

The two-dimensional numerical simulations were performed in the channels with repeated 10 obstacles. The channels used in simulation were the one-twentieth scale of the experimental equipment used by Maeda et al. [5] for BR of 0.06, 0.12 and 0.18, and the one-tenth scale for BR of 0.18. Higher obstacles disturbed the flame propagation and induced the shock waves crossing the channel, which lead to the enhancement and acceleration of the combustion reaction. A small local explosion in the unburned gas compressed by flames was observed near the seventh obstacle at one-tenth the size. Unlike the experiments by Maeda et al. [5], the flames did not transit to detonation under any conditions of the height of the obstacles despite using a reaction model because of three-dimensional effects.

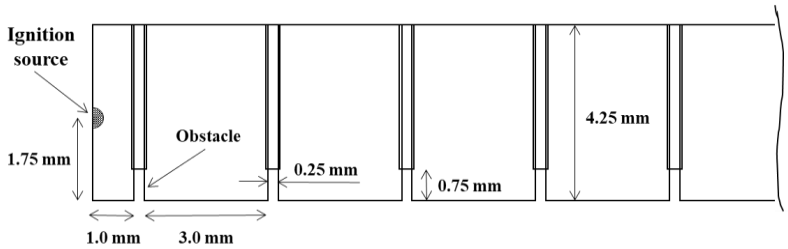

Figure 1. The frame of calculation grids for BR of 0.18 at one-twentieth the size.

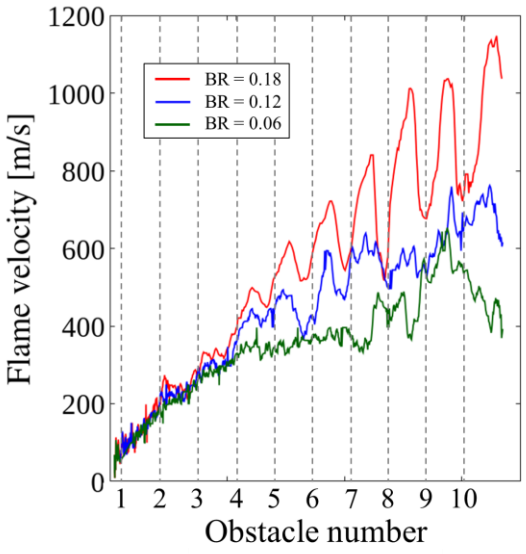

Figure 2. Flame front velocities at the position from left-side of channels which are the one-twentieth scale for various obstacle heights. Red line shows result for BR of 0.18, blue line for BR of 0.12 and green line for BR of 0.06. The broken lines in the figure show the position of obstacles.

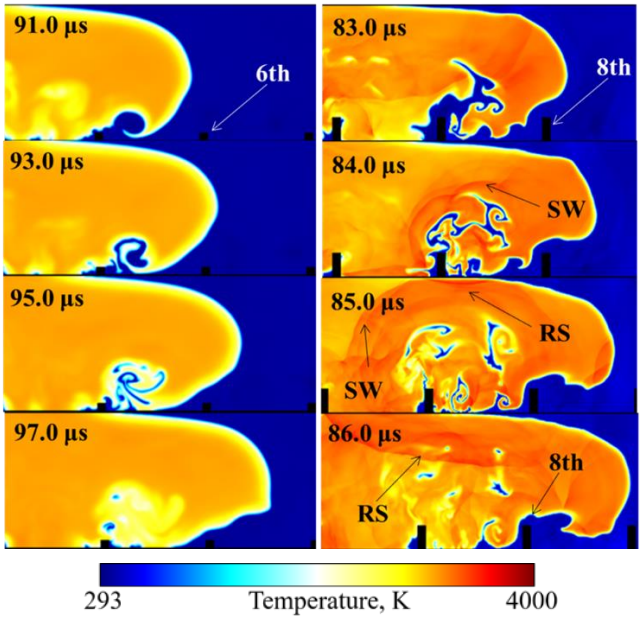

Figure 3. Temperature contours of flame propagation in channels which are one-twentieth the size. (Left) BR of 0.06, (Right) BR of 0.18, respectively.

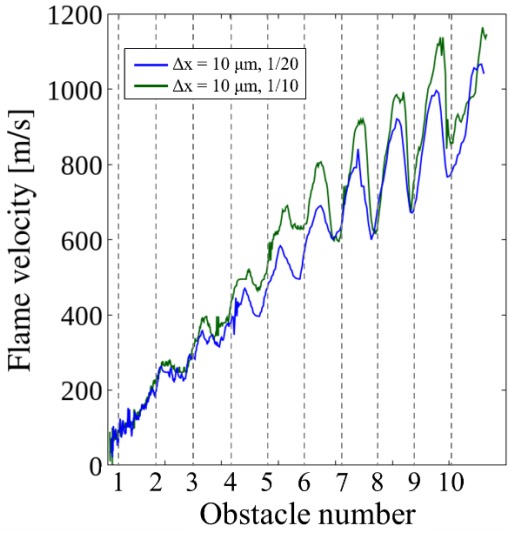

Figure 4. Flame velocities at the position from left-side at same grid width. The distance on the horizontal axis is normalized to compare with both scales. Green line shows result at the one-tenth scale and blue line at the one-twentieth scale

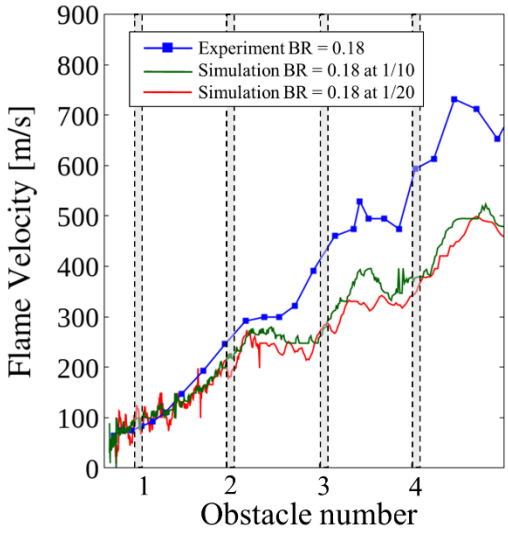

Figure. 5 Flame velocities until the fourth obstacle for BR of 0.18. Blue is experimental result [5], green is simulation at one-tenth the size and red is simulation at one-twentieth the size.

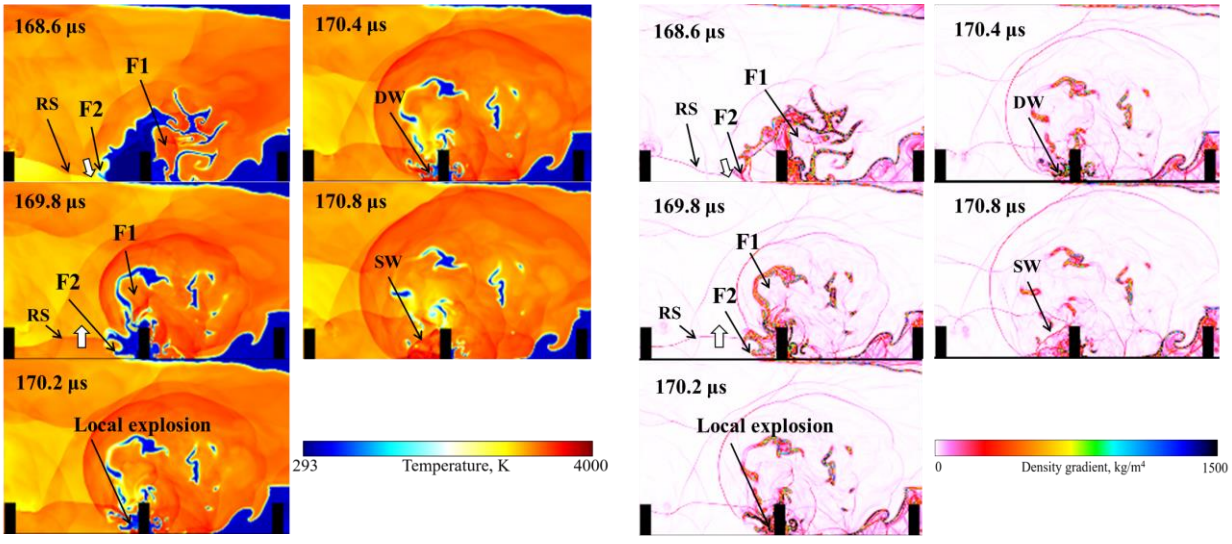

(a) (b)

Figure 5. (a)Temperature contours and (b)contour of density gradients of scene when a local explosion occurs arranged in chronological order in the channel at one-tenth the size for BR of 0.18.

Acknowledgments

The numerical simulations in this research were carried out in the Super Computing system in Osaka University. This study is also supported by Japan Nuclear Fuel Ltd. The authors are grateful to S. Maeda and T. Obara for allowing us to refer the experiment results.

References

[1]Shchlkin KI, Troshin YK. (1965). Gasdynamics of Combustion. Mono Book Corporation. p.30.

[2]Peraldi O, Knystautas R, Lee JH. (1986). Criteria for Transition to Detonation in Tubes. Proc.21st Symp. (Int.) Combust. pp. 1629-1637.

[3]Dorofeev SB, Sidorov VP, Kuznetsov MS, Matsukov ID, Alekseev VI. (2000). Effect of scale on the onset of detonations. Shock Waves. 10: 302-315.

[4]Goodwin GB, Houim RW, Oran ES. (2016). Effect of decreasing blockage ratio on DDT in small channels with obstacles. Combustion and Flame 173. 16-26.

[5]Maeda S, Minami S, Okamoto D, Obara T. (2016). Visualization of deflagration-to-detonation transitions in a channel with repeated obstacles using a hydrogen-oxygen mixture. Shock Waves. 26:573-586.

[6]Ivanov MF, Kiverin AD, Liberman MA. (2011). Hydrogen-Oxygen flame acceleration and transition to detonation in channels with no-slip walls for a detailed chemical reaction model. Physical Review E83. 056313.

[7]Ago A, Tsuboi N, Dzieminska E, Hayashi AK. (2018). Two-Dimensional Numerical Simulation of Detonation Transition with Multi-Step Reaction Model: Effects of Obstacle Height. Combustion Science and Technology.

[8] Wada Y, and Liou MS, (1997). An Accurate and Robust Flux Splitting Scheme for Shock and Contact continuities SIAM Journal on Scientific Computing. 18(3): 633-657.

[9] Van Leer B. (1979). Towards the ultimate conservative difference scheme. V. A second-order sequel to Godunov's method. Journal of Computational Physics. 32(1): 101-136.

[10] Gottlieb S, Shu CW. (1998). Total variation diminishing Runge-Kutta schemes. MATHEMATICS OF COMPUTATION. 67: 73-85.

[11] Shimizu K, Hibi A, Koshi M, Morii Y, Tsuboi N. (2011). Updated kinetic mechanism for high pressure hydrogen combustion. JOURNAL OF PROPULSION AND POWER. 27(2): 383-395.

[12] Gamezo VN, Desbordes D, Oran ES. (1999). Two-dimensional reactive flow dynamics in cellular detonation waves. Shock Waves. 9(1): 11-17.